ELSEVIER

Journal of Fluids and Structures 22 (2006) 783–791

JOURNAL OF FLUIDS AND STRUCTURES

www.elsevier.com/locate/jfs

Frequency lock-in is caused by coupled-mode flutter

E. de Langre*

Département de Mécanique, LadHyX, Ecole Polytechnique, 91128 Palaiseau, France

Received 29 September 2005; accepted 7 April 2006
Available online 24 July 2006

Abstract

The mechanism underlying the lock-in of frequencies in flow-induced vibrations is analysed using elementary linear dynamics. Considering the case of lock-in in vortex-induced vibrations (VIV), we use a standard wake oscillator model, as in previous studies, but in its simplest form where all nonlinear terms and all dissipative terms are neglected. The stability of the resulting linear system is analysed, and a range of coupled-mode flutter is found. In this range, the frequency of the most unstable mode is found to deviate from the Strouhal law when the frequency of the wake oscillator approaches that of the free cylinder motion. Simultaneously the growth rate resulting from coupled-mode flutter increases, which would lead to higher vibration amplitudes. The extent of the range of lock-in is then compared with experimental data, showing a good agreement. It is therefore stated that the lock-in phenomenon, such as in VIV, is a particular case of linear coupled-mode flutter.

Keywords: VIV; Lock-in; Flutter

1. Introduction

In the dynamics of coupled fluid-structure interaction systems, the phenomenon of frequency lock-in is often referred to. It may be defined, from a phenomenological point of view, as the observation that a frequency, in a given range of control parameters, deviates from its expected values while being close to the value of another frequency of the system.

This is typically the case in vortex-induced vibration (Williamson and Govardhan, 2004) for the shedding frequency in the wake of a bluff body: in the absence of motion of the solid, this frequency increases proportionally with the flow velocity, following the Strouhal law. When the solid is let free to vibrate transversally to the flow, a coupling between this motion and the wake dynamics exists. This results in a complex evolution of the shedding frequency, which deviates from Strouhal law as the natural frequency of the solid is approached: the wake frequency is said to lock onto that of the solid. The lock-in range is also that of large oscillatory motion of the bluff body, which is of practical importance.

Similarly, in the field of aeroacoustics, coupling may exist, such as between the acoustic modes of a cavity and the oscillating shear layer instability caused by the grazing flow over the edges of the same cavity; see Hémon et al. (2004) for instance. There, the frequency of the shear layer instability is influenced in its evolution in the vicinity of the frequency of the acoustic modes, and lock-in is observed. Many other cases exist such as in the coupling between a mixing layer instability of wind above a crop canopy and the natural frequency of the plants of the canopy (Py et al.,

*Tel.: +33 1 69 33 36 01; fax: +33 1 69 33 30 30.
E-mail address: delangre@ladhyx.polytechnique.fr.

0889-9746/$ - see front matter
doi:10.1016/j.jfluidstructs.2006.04.008

2004, 2006). More generally a frequency lock-in may appear whenever an oscillating instability is coupled with an oscillating system.

The most commonly accepted interpretation of the mechanism underlying frequency lock-in is that of resonance. In the case of vortex-induced vibration this reads as follows: as the frequency of the unstable system (the wake) approaches that of the oscillator (the bluff body), the oscillating lift force causes an increasing amplitude of motion, by a standard resonance effect. Then, provided this amplitude is large enough, the wake is somehow affected and forced to move at the natural resonating frequency of the solid. This feedback mechanism is implicitly assumed to be nonlinear, as the existence of lock-in and its extent depend on the amplitude of motion.

In terms of modelling of the coupling between an oscillating wake and an oscillating bluff body, many qualitative and some quantitative aspects can be represented by using the simple concept of a wake oscillator, following Hartlen and Currie (1970); see Facchinetti et al. (2002, 2004a,b). In such models the wake dynamics is lumped in only one variable that follows a simple equation such as van der Pol's. This is sufficient to have a self-sustained oscillation with a limit cycle. The bluff body is then considered as another oscillator excited by the wake variable. Conversely the effect of the motion of the solid on the wake is represented by a forcing on the van der Pol equation. Facchinetti et al. (2004a) have shown that the most appropriate forcing is proportional to the acceleration of the bluff body. Using this nonlinear coupled model some main features of the VIV phenomenology can be retrieved. In particular, the extension of lock-in and its dependence on the mass ratio are well described. The model has then been extended to three-dimensional applications such as in vortex-induced waves propagating along cables (Facchinetti et al., 2004b; Mathelin and de Langre, 2005).

Still, some aspects of the mechanism underlying frequency lock-in remain unclear: how is the range of lock-in affected by the parameters of the system? How is the evolution of frequencies during lock-in affected by these same parameters? More generally, is the mechanism of frequency lock-in essentially linear or nonlinear? In order to answer these questions, the wake oscillator model used in Facchinetti et al. (2004a,b) is now simplified to its elementary terms.

2. Elementary mechanism of lock-in

2.1. The coupled nonlinear model

We recall here the main features of the nonlinear model used by Facchinetti et al. (2004a), coupling a cylinder motion, $Y(T)$ and a wake oscillation $q(T)$, where T is time. The dynamics of the displacement of the cylinder is simply that of a linear oscillator, affected by the fluid loading,

$$(m_S + m_F)\ddot{Y} + (r_S + r_F)\dot{Y} + hY = S, \tag{1}$$

where m_S, r_S and h are, respectively, the mass, damping and stiffness of the cylinder motion in the absence of fluid, and dots representing differentiation with respect to time. The fluid loading is found in the added mass, m_F, the added damping, r_F, and the forcing by the oscillating wake, S. These terms are related to the variables in the fluid by

$$m_F = \frac{1}{4}\pi\rho D^2 C_M, \quad r_F = 2\pi S_T \frac{U}{D}\gamma\rho D^2, \quad S = \frac{1}{4}\rho U^2 D C_{L0} q, \tag{2}$$

where D is the diameter of the cylinder, ρ is the fluid density, $C_M = 1$ is the added mass coefficient, S_T is the Strouhal number, U is the flow velocity, $\gamma = C_D/(4\pi S_T)$ is a parameter depending on the drag coefficient C_D, and finally C_{L0} is the fluctuating lift coefficient.

The dynamics of the wake follows a van der Pol equation

$$\ddot{q} + \varepsilon\left(2\pi S_T \frac{U}{D}\right)(q^2 - 1)\dot{q} + \left(2\pi S_T \frac{U}{D}\right)^2 q = \frac{A}{D}\ddot{Y}, \tag{3}$$

where ε and A are parameters which can be derived from simple experimental data on the wake dynamics itself, typically $\varepsilon = 0.3$ and $A = 12$ (Facchinetti et al., 2004a). Here the variable q is defined as $q(t) = 2C_L(t)/C_{L0}$, where $C_L(t)$ is the instantaneous lift coefficient.

These coupled nonlinear equations, Eqs. (1) and (3), can be put in an appropriate dimensionless form by using the time scale of the natural oscillation of the cylinder in still fluid. The dimensionless variables read

$$t = \sqrt{\frac{h}{m_S + m_F}}T, \quad y = \frac{Y}{D}, \tag{4}$$

so that Eqs. (1) and (3) now read

$$\ddot{y} + \lambda\dot{y} + y = M\Omega^2 q, \quad \ddot{q} + \varepsilon\Omega(q^2 - 1)\dot{q} + \Omega^2 q = A\ddot{y}, \tag{5}$$

where $\Omega = S_T U_R$ is the dimensionless frequency of a self-sustained oscillation of the wake, $U_R = U/(fD)$ being the reduced velocity, the damping coefficient λ standing for all damping terms acting on the cylinder, and M is a mass parameter. They read

$$\lambda = 2\xi + \frac{\gamma}{\mu}\Omega, \quad M = \frac{C_{L0}}{2}\frac{1}{8\pi^2 S_T^2 \mu}, \quad \mu = \frac{m_S + m_F}{\rho D^2}. \tag{6}$$

Note that this dimensionless form differs from that used by Facchinetti et al. (2004a,b), as we use here the frequency of the cylinder motion as a reference, instead of the frequency of the wake.

2.2. A linear model

In order to point out the mechanism underlying the evolution of the frequency of the coupled system, we now disregard several terms in Eq. (5). The only nonlinear term of this set of equations is that of the van der Pol oscillator, $\varepsilon\Omega q^2\dot{q}$. Its role in setting the amplitude of the limit cycle of the coupled system is essential, but we now assume that it does not significantly affect the frequency. Similarly the linear negative damping term in the same van der Pol equation, $-\varepsilon\Omega\dot{q}$, is essential in providing a self-excited amplification of the wake variable, modelling the naturally unstable wake, but we assume that it does not play an important role in setting the frequency. Finally, the positive damping term in the cylinder equation, $\lambda\dot{y}$, also plays a role in the development of the coupled dynamics, but not on the resulting frequency. These three terms can be assumed to play a negligible role in the evolution of the frequencies because of the typical range of values of the parameters ε and λ (Facchinetti et al., 2004a). Neglecting these three terms, Eq. (5) reduces to

$$\ddot{y} + y = M\Omega^2 q; \quad \ddot{q} + \Omega^2 q = A\ddot{y}. \tag{7}$$

Here, the two linear undamped oscillators are coupled in the same way the damped cylinder oscillator and the van der Pol oscillator for the wake were coupled in Eq. (5). The only remaining control parameter is now the frequency Ω, which is proportional to the flow velocity $\Omega = S_T U_R$, the dimensionless mass M depending on the mass ratio, fluctuating lift and Strouhal number, Eq. (6).

2.3. Coupled-mode flutter

The solution of Eq. (7) is straightforward. Considering modes $(y, q) = (y_0, q_0)\mathrm{e}^{\mathrm{i}\omega t}$ yields the frequency equation

$$\mathbf{D}(\omega) = \omega^4 + [(AM - 1)\Omega^2 - 1]\omega^2 + \Omega^2 = 0. \tag{8}$$

We consider first the case where $AM < 1$, which is illustrated in Fig. 1 for $AM = 0.5$. Depending on the value of Ω, the system is neutrally stable or unstable.

When $\Omega < 1/(1 + \sqrt{AM})$ or $\Omega > 1/(1 - \sqrt{AM})$, two neutrally stable modes exist, which are defined, respectively, by their real frequencies such that

$$2(\omega_\pm)^2 = 1 + (1 - AM)\Omega^2 \pm ([1 + (1 - AM)\Omega^2]^2 - 4\Omega^2)^{1/2}. \tag{9}$$

These modes may be attributed to the wake dynamics, noted "W" in Fig. 1(a), and to the solid dynamics, noted "S", by simply considering their mode shape: Eq. (7) yields

$$\frac{y_0}{q_0} = \frac{M\Omega^2}{1 - \omega^2} = \frac{\Omega^2 - \omega^2}{A\omega^2}, \tag{10}$$

so that the mode with the frequency closer to the line $\omega_R = \Omega$ in Fig. 1(a) is the wake mode and the mode closer to the line $\omega_R = 1$ is the solid mode. In each mode, except at $\Omega = 0$, both components y and q exist, though one is clearly dominant.

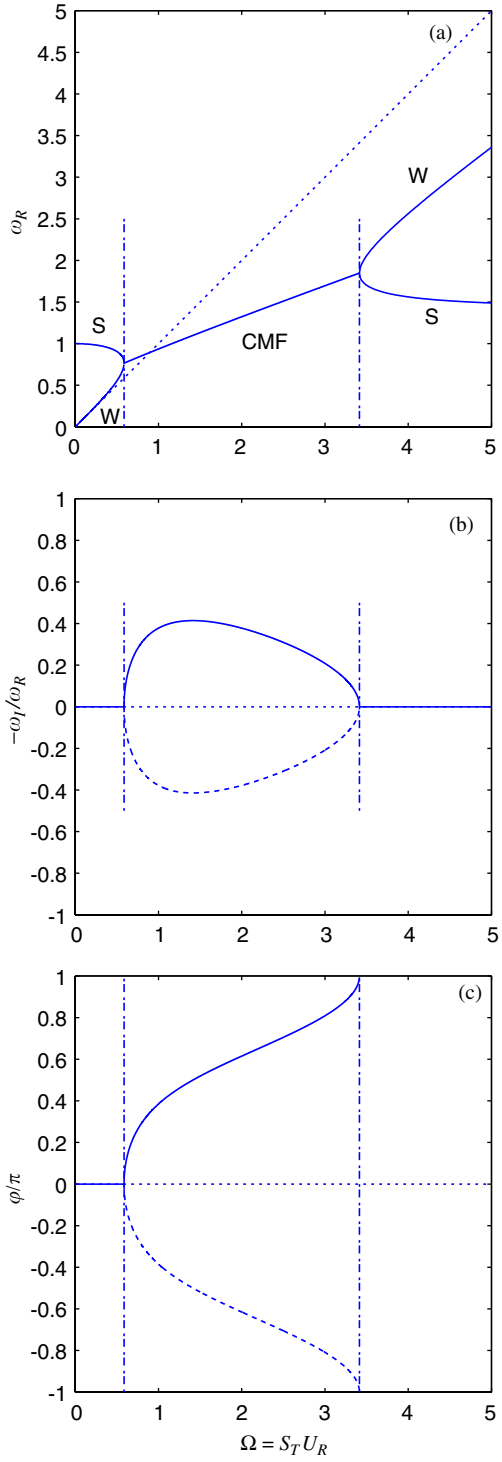

Fig. 1. Effect of the dimensionless flow velocity $\Omega = S_T U_R$ on the modes of the coupled system defined by Eq. (7), for $AM = 0.5$: (a) frequency, (b) growth rate, (c) phase between the lift q and the displacement y. —, Unstable mode; - -, damped mode; $- \cdot -$, limit of the range of lock-in; $\cdots$, wake mode of the uncoupled solution at $AM = 0$, where $\omega_R = \Omega$, $\omega_I = 0$. In (a), S denotes a solid mode, W a wake mode and CMF a coupled-mode flutter solution.

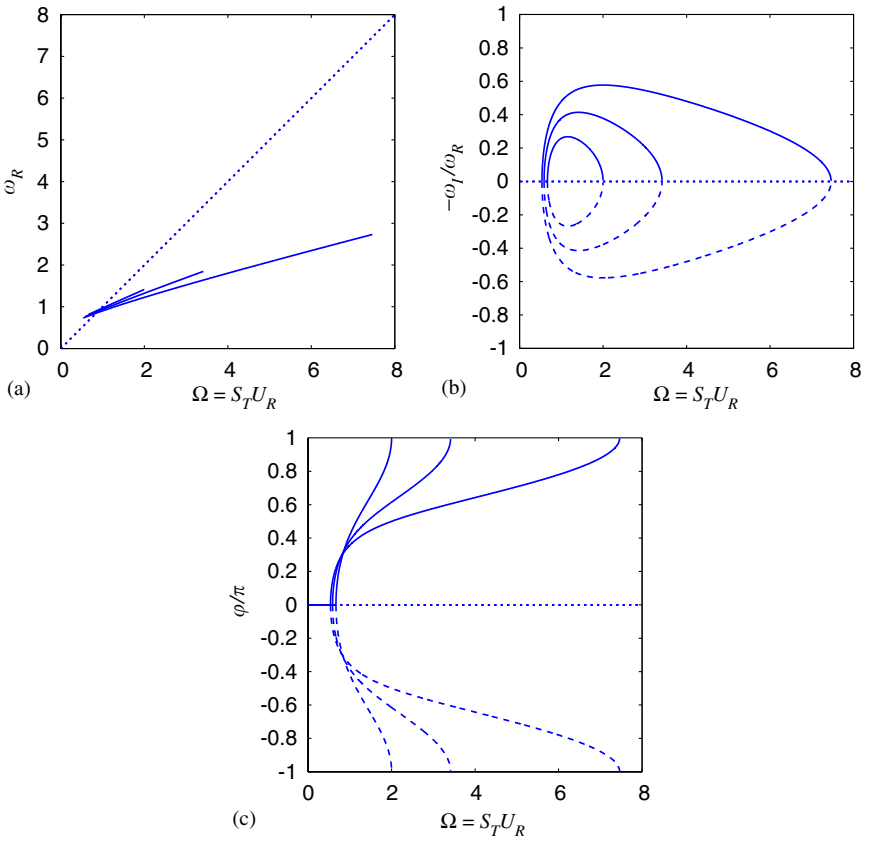

Fig. 2. Influence of the combined mass parameter AM on the characteristics of lock-in: (a) frequency, (b) growth rate, (c) phase between the lift q and the displacement y. In each plot the results for three values of AM are shown, 0.25, 0.50 and 0.75, this being the order of increasing lock-in range. —, Unstable mode; - -, damped mode; ⋯, wake mode of the uncoupled solution at $AM = 0$.

In the range $1/(1+\sqrt{AM}) < \Omega < 1/(1-\sqrt{AM})$ two modes exist, but with complex conjugate frequencies, such that

$$\omega_{\pm} = \left[\frac{\Omega}{1+\tan^2\theta}\right]^{1/2}(1 \pm \mathrm{i}\tan\theta), \tag{11}$$

where

$$\theta = \frac{1}{2}\arctan\frac{[4\Omega^2 - (1+(1-AM)\Omega^2)^2]^{1/2}}{1+(1-AM)\Omega^2}. \tag{12}$$

This type of solution is commonly referred to as coupled-mode flutter (Blevins, 1990; Schmid and de Langre, 2003), denoted by "CMF" in Fig. 1(a), which displays the merging of the two frequencies of the two neutral modes, leading to a range of instability. One of these two modes is unstable ($\omega_I < 0$), the other being damped, Fig. 1(b). As the frequency Ω is further increased, a decoupling occurs and two neutral modes reappear. The phase between the lift q and the displacement y, Fig. 1(c), switches from 0 to π in this range of coupled-mode flutter. In this range, no distinction can be made between a solid and a wake mode. A new regime arises, where a coupled motion with a phase shift allows a nonconservative cycle to exist, which is the cause of the instability. The range of coupled-mode flutter may be considered as a range of lock-in because the frequency of the wake mode strongly deviates from the relation $\omega = \Omega$, and follows a relation where the natural frequency of the solid, $\omega = 1$, plays a role. Moreover, in this region an unstable mode appears, which will introduce dynamics different from that of the pure wake or solid modes.

The only parameter affecting the range of lock-in, as well as the magnitude of the deviation in frequency is the combined parameter AM. In Fig. 2 we vary its value from 0.25 to 0.75. The extent of lock-in is found to increase

steadily, mainly in its upper bound. The growth rate and damping of the modes, as well as the phase, are very similar to the case where $AM = 0.5$.

2.4. Selection of the dominant mode

In the range of lock-in, we may state that the motion in y and q that emerges from any perturbation of the system is dominated by the unstable mode. Its oscillating frequency is given by the real part in Eq. (11),

$$\omega_R = \left(\frac{\Omega}{1+\tan^2\theta}\right)^{1/2}. \tag{13}$$

Outside the lock-in range we found that two neutral modes coexist. In the simplest model used here these modes are neutrally stable because all damping terms, positive or negative, have been neglected. In practice, because of the natural instability of the wake, $\varepsilon>0$, and because of the damping of the solid motion, $\lambda>0$, each mode is either damped or unstable, and the motion will be dominated by the unstable mode. This can be investigated by taking into account the two damping terms, so that Eq. (5) becomes

$$\ddot{y} + \lambda\dot{y} + y = M\Omega^2 q, \quad \ddot{q} - \varepsilon\Omega\dot{q} + \Omega^2 q = A\ddot{y}. \tag{14}$$

The corresponding frequency equation reads

$$\mathbf{D}(\omega;\varepsilon,\lambda) = (1 + \mathrm{i}\lambda\omega - \omega^2)(\Omega^2 - \mathrm{i}\varepsilon\Omega\omega - \omega^2) - AM\omega^2\Omega^2 = 0. \tag{15}$$

The effect of the parameters λ and ε on the modes of the system can be assessed by considering the variation of the eigenfrequencies ω with these parameters. Though they are of finite magnitude, typically $\varepsilon = 0.3$ and $\lambda = 0.1$, a simple first order expansion is made following Peake (1997) by setting

$$\omega = \omega_0 + \varepsilon\omega_\varepsilon + \lambda\omega_\lambda, \tag{16}$$

where ω_0 satisfies the frequency equation without λ and ε, so that

$$\mathbf{D}(\omega_0;0,0) = 0. \tag{17}$$

The expansion of Eq. (15) reads

$$\mathbf{D}(\omega_0 + \varepsilon\omega_\varepsilon + \lambda\omega_\lambda;\varepsilon,\lambda) = D(\omega_0;0,0) + \varepsilon\omega_\varepsilon\frac{\partial D}{\partial\omega} + \lambda\omega_\lambda\frac{\partial D}{\partial\omega} + \varepsilon\frac{\partial D}{\partial\varepsilon} + \lambda\frac{\partial D}{\partial\lambda} = 0. \tag{18}$$

This implies that the sought variations ω_ε and ω_λ satisfy, respectively,

$$\omega_\varepsilon = -\frac{\partial D/\partial\varepsilon}{\partial D/\partial\omega}, \quad \omega_\lambda = -\frac{\partial D/\partial\lambda}{\partial D/\partial\omega}; \tag{19}$$

all derivatives being taken at the reference state $(\omega_0, 0, 0)$. These derivatives can be easily derived from Eq. (15), so that the effect of the two parameters λ and ε on the frequency ω is, at the first order in λ, ε,

$$\omega = \omega_0 + \mathrm{i}\varepsilon\left[\Omega\omega_0^2\frac{(1-\omega_0^2)}{2(\omega_0^4-\Omega^2)}\right] - \mathrm{i}\lambda\left[\omega_0^2\frac{(\Omega^2-\omega_0^2)}{2(\omega_0^4-\Omega^2)}\right]. \tag{20}$$

By considering the sign of the imaginary part of the frequency when ω_0 is either the frequency of the wake mode or that of the solid mode, it appears that both parameters have a destabilizing effect on the wake mode and a damping effect on the solid mode. This is illustrated in Fig. 3 where the effects of both parameters are shown independently, on the frequencies and on the growth rate, using Eq. (20). In both cases the most unstable mode has the frequency of the wake mode outside the range of lock-in.

The resulting frequency of oscillation that can therefore be expected for such a system is shown in Fig. 4, where only the dominant mode is shown. For small values of AM, lock-in is a small deviation of the evolution of the frequency of the original wake mode, in a limited range of reduced velocity U_R. For larger values of AM, a larger range of U_R is affected even outside the range of coupled-mode flutter.

2.5. Critical mass ratio

The extent of lock-in, in terms of reduced flow velocity, is known to be significantly affected by the mass ratio between the fluid and the solid systems. In our simple linear model, the upper and lower limit of lock-in, which is here

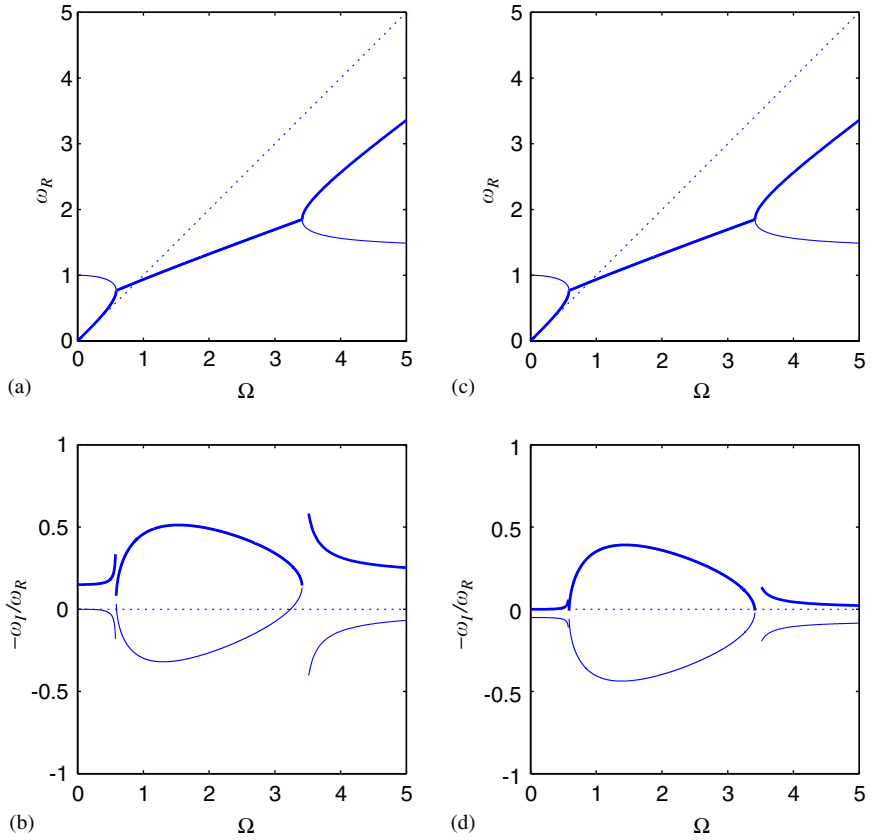

Fig. 3. Selection of the dominant mode by the effect of damping on the growth rate of the modes of the coupled system, $AM = 0.5$, using Eq. (20). (a) and (b) Effect of the negative damping of the wake equation, $\varepsilon = 0.3$ and $\lambda = 0$; (c) and (d) effect of the damping of the cylinder, $\varepsilon = 0$ and $\lambda = 0.1$. In (a) and (c) the frequency of the most unstable mode is shown in bold lines, corresponding to the highest growth rate in (b) and (d), respectively.

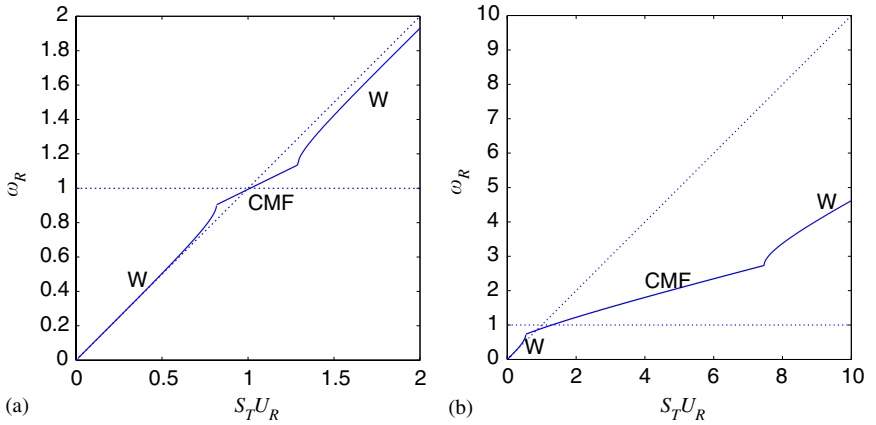

Fig. 4. Effect of the flow velocity $\Omega = S_T U_R$ on the frequency of the dominant mode of the coupled system. (a) $AM = 0.05$, the frequency deviates from Strouhal law only near $\Omega = 1$, by coupled mode flutter. (b) $AM = 0.75$ the frequency deviates from Strouhal law in a large range of coupled mode flutter, and is also affected outside this range. —, Frequency; ⋯, uncoupled solution; W, wake mode; CMF, coupled-mode flutter.

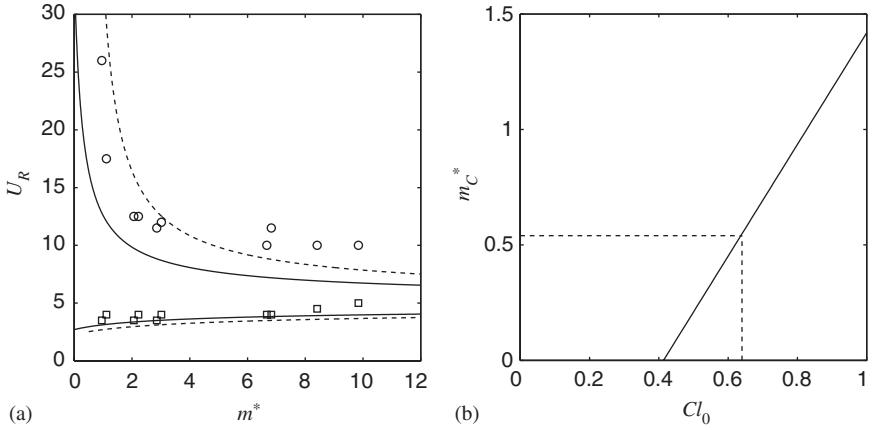

Fig. 5. Lock-in at low mass ratio m^*. (a) Effect of the mass parameter m^* on the upper and lower limits of lock-in, expressed here in reduced velocity U_R, with $C_{L0} = 0.3$ (—) and $C_{L0} = 0.6$ (- -); □, lower limit; o, upper limit in experiments by Govardhan and Williamson (2000); see also Facchinetti et al. (2004a). (b) Effect of the unsteady lift coefficient on the critical mass ratio below which lock-in persists for high reduced velocities: —, Eq. (24); - -, critical value $m_C^* = 0.54$ given by Govardhan and Williamson (2000), corresponding to $C_{L0} = 0.64$.

coupled-mode flutter, are respectively,

$$\Omega^{\mathrm{Min}} = \frac{1}{1+\sqrt{AM}}, \quad \Omega^{\mathrm{Max}} = \frac{1}{1-\sqrt{AM}}. \tag{21}$$

This can also be expressed in terms of the relation between the reduced velocity U_R and the mass ratio m^*, defined by

$$U_R = \frac{\Omega}{S_T}, \quad m^* = \frac{m_S}{(\pi/4)\rho D^2} = \frac{4}{\pi}\mu - C_M. \tag{22}$$

We have then a closed form relation between these parameters

$$S_T U_R^{\mathrm{Min}} = \left[1 + \sqrt{\frac{AC_{L0}}{4\pi^3 S_T^2 (m^* + C_M)}}\right]^{-1}, \quad S_T U_R^{\mathrm{Max}} = \left[1 - \sqrt{\frac{AC_{L0}}{4\pi^3 S_T^2 (m^* + C_M)}}\right]^{-1}. \tag{23}$$

These limits only depend on the mass ratio m^*, the Strouhal number S_T and the lift coefficient C_{L0}. Their evolutions are plotted on Fig. 5(a), for $S_T = 0.2$ and two values of C_{L0}. Experimental data on these limits, from Govardhan and Williamson (2000), are well approximated. When the mass ratio is varied, the lower limit is not much affected, while the upper limit increases significantly near $m^* = 1$, as also found in the experiments. Depending on the value of the lift parameter C_{L0}, a critical value, denoted m_C^*, exists, at which lock-in persists up to infinite reduced velocity. Using Eq. (23), this critical value is

$$m_C^* = \frac{AC_{L0}}{4\pi^3 S_T^2} - C_M. \tag{24}$$

Fig. 5(b) illustrates the influence of the lift coefficient C_{L0} on this critical value. At $C_{L0} = 0.3$, no limit exists, though the upper value of U_R is quite high at $m^* = 0$. To obtain a critical mass parameter of $m_C^* = 0.54$, as reported by Govardhan and Williamson (2002), a lift coefficient $C_{L0} = 0.64$ approximately is needed, which is not outside the range of values reported in the literature.

3. Discussion

This linear model does not directly provide predictions of the amplitude of motion of the cylinder. Yet, the high growth rate that results from coupled-mode flutter is clearly the energy source needed to cause high amplitude of motion in this range. The amplification of motion at lock-in, observed in experiments, can therefore be understood as the consequence of an amplification of energy input, which results in a higher saturated amplitude when nonlinear effects are introduced. This interpretation is consistent with the analysis of the evolution of phase in the lock-in range.

The linear coupled mode flutter model therefore provides an interpretation for both the frequency evolution and for the amplification of cylinder motion in the range of lock-in. Moreover, the extent of lock-in and in particular the increase of the upper limit at low mass ratios is predicted.

Coupled-mode flutter in flow-induced vibration is often illustrated by the simple case of the plunge-torsion instability of airfoils (Blevins, 1990). Here flutter occurs by coupling between the transverse displacement y and the wake variable q. The latter, which is actually the fluctuating lift, is in some cases related to the rotation of the position of the separation points on the cylinder. Then the equivalent of torsion in this coupled-mode flutter would be the rotation of the near wake.

The model proposed here, to show that the mechanism underlying lock-in is essentially a case of linear coupled-mode flutter, is a degenerate form of the nonlinear wake oscillator models used in previous studies. Though not all the complex dynamics of VIV can be modelled by such oscillator models, it appears that some essential mechanisms do not require more sophisticated models. This conclusion was for instance reached in Facchinetti et al. (2004a,b) when using a simple van der Pol oscillator for the wake. The results shown in the present paper suggest that some underlying mechanisms in VIV may actually be even simpler than originally thought: if the lock-in effect can be understood in several of its characteristics, such as its extent and the phase evolution, by a linear model of coupled-mode flutter, the more advanced concepts of resonance with a nonlinear feedback do not need to be invoked.

Other aspects of VIV may also be analysed using this linear approach. If one considers that the effect of the cylinder motion of the wake is not exactly in phase with the acceleration, the evolution of the frequency of the most unstable mode is more complex: the deviation from Strouhal law, as well as the corresponding growth rates show evolutions which are similar to those observed in the transition between 2P and 2S modes.

References

Blevins, R.D., 1990. Flow-Induced Vibrations. Van Nostrand Reinhold, New York.

Facchinetti, M.L., de Langre, E., Biolley, F., 2002. Vortex shedding modeling using diffusive van der Pol oscillators. Comptes Rendus Mécanique 330, 451–456.

Facchinetti, M.L., de Langre, E., Biolley, F., 2004a. Coupling of structure and wake oscillators in vortex-induced vibrations. Journal of Fluids and Structures 19 (3), 123–140.

Facchinetti, M.L., de Langre, E., Biolley, F., 2004b. Vortex-induced travelling waves along a cable. European Journal of Mechanics B/Fluids 23, 199–208.

Govardhan, R., Williamson, C.H.K., 2000. Modes of vortex formation and frequency response of a freely vibrating cylinder. Journal of Fluid Mechanics 420, 85130.

Govardhan, R., Williamson, C.H.K., 2002. Resonance forever: existence of a critical mass and an infinite regime of resonance in vortex-induced vibration. Journal of Fluids Mechanics 473, 147–166.

Hartlen, R., Currie, I., 1970. Lift-oscillator model of vortex-induced vibration. ASCE Journal of the Engineering Mechanics Division 96, 577–591.

Hémon, P., Santi, F., Amandolèse, X., 2004. On the pressure oscillations inside a deep cavity excited by a grazing flow. European Journal of Mechanics B/Fluids 23, 617–632.

Mathelin, L., de Langre, E., 2005. Vortex-induced vibrations and waves under shear flow with a wake oscillator model. European Journal of Mechanics B/Fluids 24, 478–490.

Peake, N., 1997. On the behavior of a fluid-loaded cylindrical shell with mean flow. Journal of Fluid Mechanics 338, 347–410.

Py, C., de Langre, E., Moulia, B., 2004. The mixing layer instability of wind over a flexible crop canopy. Comptes-Rendus Mécanique 332, 613–618.

Py, C., de Langre, E., Moulia, B., 2006. A frequency lock-in mechanism in the interaction between wind and crop canopies. Journal of Fluid Mechanics, in press.

Schmid, P.J., de Langre, E., 2003. Transient growth before coupled-mode flutter. Journal of Applied Mechanics 70, 894–901.

Williamson, C.H.K., Govardhan, R., 2004. Vortex-induced vibrations. Annual Review of Fluid Mechanics 36, 413–455.